Early-Times Yang-Mills Dynamics and the Characterization of Strongly Interacting Matter with Statistical Learning

Matthew Heffernan[1], Charles Gale,[1] Sangyong Jeon[1], and Jean-François Paquet[2,3]

[1]*Department of Physics, McGill University, Montréal, Quebec H3A 2T8, Canada*
[2]*Department of Physics and Astronomy, Vanderbilt University, Nashville, Tennessee 37235, USA*
[3]*Department of Mathematics, Vanderbilt University, Nashville, Tennessee 37235, USA*

In ultrarelativistic heavy-ion collisions, a plasma of deconfined quarks and gluons is formed within 1 fm/c of the nuclei's impact. The complex dynamics of the collision before $\approx$1 fm/c is often described with parametric models, which affect the predictivity of calculations. In this work, we perform a systematic analysis of LHC measurements from Pb-Pb collisions, by combining an *ab initio* model of the early stage of the collisions with a hydrodynamic model of the plasma. We obtain state-of-the-art constraints on the shear and bulk viscosity of quark-gluon plasma. We mitigate the additional cost of the *ab initio* initial conditions by combining Bayesian model averaging with transfer learning, allowing us to account for important theoretical uncertainties in the hydrodynamics-to-hadron transition. We show that, despite the apparent strong constraints on the shear viscosity, metrics that balance the model's predictivity with its degree of agreement with data do not prefer a temperature-dependent specific shear viscosity over a constant value. We validate the model by comparing with discriminating observables not used in the calibration, finding excellent agreement.

Introduction.—The fundamental degrees of freedom of quantum chromodynamics (QCD)—the theory of the nuclear strong interaction—are quarks and gluons. In the overlap region of two heavy nuclei colliding at ultra-relativistic energies, a dense plasma of such quarks and gluons is formed [1]. The rapid expansion of this strongly interacting plasma can be described with relativistic viscous hydrodynamics [2–5], providing a window into the transport properties of hot and dense nuclear matter. This theoretical development brought the heavy-ion program into a characterization phase.

Early analyses of measurements at the Relativistic Heavy Ion Collider established that the specific shear viscosity η/s (the coefficient of shear viscosity over the entropy density) of quark-gluon plasma must be small, of the order of $1/4\pi$ [6]. Since these early analyses, considerable effort has been devoted to quantifying the full temperature dependence of both shear and bulk viscosity [2]. This is a formidable undertaking, since the quark-gluon plasma is formed in heavy-ion collisions for less than 10^{-23} sec (10 Fermi/c), evolving through multiple distinct stages between the impact of the nuclei and the final measurement of particle showers by the detectors. Furthermore, it was understood early on that shortcomings in the theoretical understanding of any stage of the collision translate into uncertainties in the determination of the viscosities [7]. An important development has been the use of Bayesian methods to quantify precisely the uncertainties on the viscosities extracted from model-to-data comparisons. A number of Bayesian analyses have now been performed [8–20], comparing modern multistage models of heavy-ion collisions with broad sets of measurements from the Relativistic Heavy Ion Collider and the Large Hadron Collider.

A long-standing source of uncertainty in heavy-ion collisions is the early stage of the collision, which provides the initial conditions for the relativistic viscous fluid dynamic simulation. While multiple early-stage models have been studied and compared in the literature, current Bayesian analyses have mostly relied on a flexible parametric model of the impact of the collision [21], sometimes augmented with more parameters [20] or supplemented with simplified dynamical models of the early stage of the collision [15,17,20]. In this work, we replace this parametric approach with an *ab initio* model of the early stage of the collision, the IP-Glasma model [22,23]. The foundation of the IP-Glasma model is to describe the nuclei, before their collision, as two color glass condensates, which is a limiting representation of the low-energy gluons in large nuclei accelerated at high energies [24]. The collision of the two color glass condensates generates gluon fields [25,26] which are evolved in time with the classical Yang-Mills equations. This model is known for its success in describing a wide range of heavy-ion measurements with a limited set of parameters [2,23,27–32].

Using these *ab initio* IP-Glasma initial conditions, we show in this work that our state-of-the-art model of heavy-ion collisions can describe a wide set of heavy-ion measurements. We employ Bayesian techniques to constrain the parameters in our approach, including shear and bulk specific viscosity coefficients. We also illustrate the

power of transfer learning to account for uncertainty from modeling choices in simulations of heavy-ion collisions. This paper is a companion paper to a larger one [33] that contains many of the details omitted here for brevity.

Model-data comparison.—We consider a broad range of measurements from Pb-Pb collisions with $\sqrt{s_{\mathrm{NN}}} = 2.76$ TeV center-of-mass energy per nucleon pair at the Large Hadron Collider [33]: (i) the number of charged hadrons per unit pseudorapidity $dN_{ch}/d\eta$ [34], (ii) the number of identified charged hadrons per unit rapidity dN_i/dy, $i \in \{\pi, p, k\}$ [35], (iii) the transverse energy per unit pseudorapidity $dE_T/d\eta$ [36], (iv) the mean transverse momenta of identified hadrons $\langle p_T \rangle_i$, $i \in \{\pi, K, p\}$ [35], (v) transverse momentum fluctuations $\delta p_T/\langle p_T \rangle$ [37], (vi) two-particle radial Fourier coefficients [38], (vii) four-particle transverse Fourier coefficient $v_2\{4\}$ [39], (viii) event plane correlators [40,41], (ix) nonlinear response coefficients that quantify mixing between higher and lower-order modes $\chi_{n,mk}$ [41], and (x) linear and nonlinear flow modes [41]. These observables represent a diverse set of the available measurements that can be calculated with reasonable statistical accuracy. Additional observables are used to verify the model's predictivity, as discussed below.

The Pb-Pb collisions are simulated in three distinct phases. The *ab initio* IP-Glasma model describes the first stage of the collision, from the nuclei's impact to the resulting production of color fields and their subsequent initial evolution. The energy-momentum tensor of these gluons is then used as initialization for relativistic viscous hydrodynamics [42–44]. Because we focus on measurements made at midrapidity, we assume boost invariance along the collision axis [45]. An equation of state based on lattice quantum chromodynamics calculations is used in the hydrodynamic phase [46–48]. The viscosities of the plasma are parametrized with the same flexible parametrizations as used in Refs. [15,49,71]. Finally, at a chosen local energy density, the energy-momentum tensor of the fluid is matched to hadronic momentum distributions, and relativistic hadronic transport [51] is used for the third phase of the collision. There is uncertainty in determining the hadronic momentum distributions at this transition, and in consequence two different models are studied: one based on Grad's 14-moment approximation of the Boltzmann equation [52–59], and the other using a Chapman-Enskog expansion in the relaxation time approximation [60–62].

Two parameters are associated with the initial IP-Glasma phase: the first relates the density of color charges and the scale at which gluon saturation occurs; the second is the hydrodynamic initialization time. Eight more parameters are used to describe the temperature dependence of the viscosities (see previous footnote), and one final parameter is used to define the energy density for the transition between hydrodynamics and hadronic transport. The smaller number of parameters in the first stage of the collision, at least four fewer parameters than previous

analyses, leads to a total of 11 parameters. We discuss later that the number of parameters can be further reduced to 8 by curtailing the flexibility of the shear viscosity parametrization.

Model-to-data comparison is performed with Bayesian inference. To access the model's predictions for different values of viscosities and other parameters, we build a fast surrogate using Gaussian process emulators. We define the admissible range of the model parameters using generalized normal priors, and we sample 350 sets of parameters with a maximum projection latin hypercube [63]. Model simulations are performed for all 350 parameter sets. Rather than training a surrogate model for each observable of interest, a dimensional reduction using principal component analysis is performed on the observables. We then train Gaussian processes on 20 principal components, which capture 90.6% of the model's information, and use these to emulate the model's output for all observables.

The above emulation is performed on calculations that use the Grad's 14-moment model to describe the transition between hydrodynamics and hadronic transport. Because of the uncertainty in this transition, it is important to use more than one model to compare with measurements. Repeating the entire procedure for our second model (Chapman-Enskog) would have been inefficient, however, given that only a single part of the model is changed. This is a general challenge in studying theoretical uncertainties in heavy-ion collision modeling: it is a high priority for the community to quantify model uncertainties, but the computational costs are often prohibitive. We address this problem with transfer learning, building upon Ref. [64]. We write the model's output as

$$f_{\text{Chapman-Enskog}}(x) = \rho f_{\text{Grad}}(x) + \delta(x) \qquad (1)$$

where ρ and δ are respectively a linear correlation term and a discrepancy term between the source (Grad) and target (Chapman-Enskog) models. Constraints on ρ and $\delta(x)$ are obtained by comparing with 50 design points evaluated with the Chapman-Enskog model. This technique allows us to estimate, at a substantially reduced computational cost, the uncertainty in the transition from hydrodynamics to individual hadrons. We emphasize the potential of this approach to study a wider range of theoretical uncertainties in the study of heavy-ion collisions. Additional details of the implementation of transfer learning and emulation can be found in Ref. [33].

We use a Gaussian likelihood function to compare models and measurements [33]. We evaluate the posterior $p(H|d, I)$, given by the product of the prior $p(H, I)$ and the likelihood $p(d|H, I)$, normalized by the Bayes evidence $p(d, I)$:

$$p(H|d, I) = \frac{p(H, I)p(d|H, I)}{p(d, I)}. \qquad (2)$$
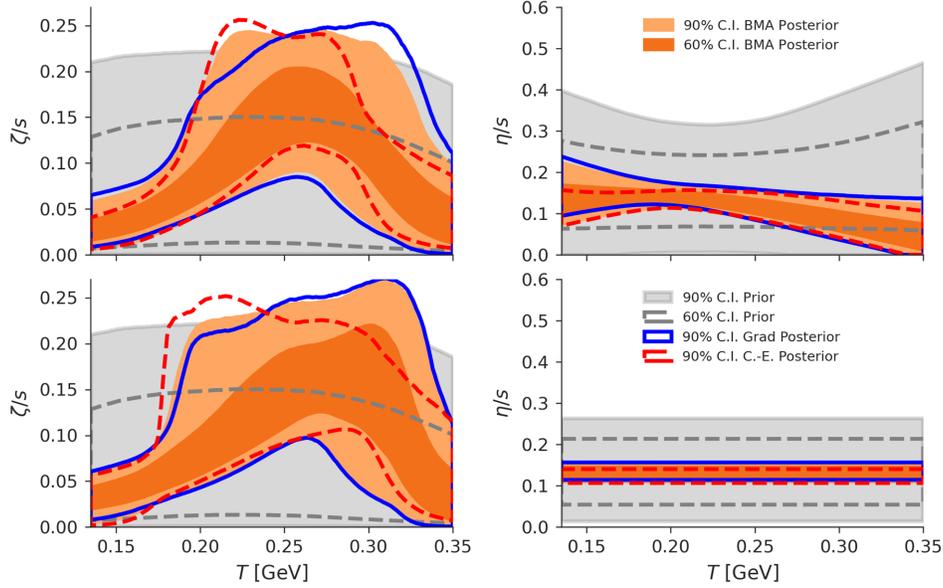
FIG. 1. Bayes model averaged viscous posterior with shear viscosity allowed to vary with temperature (top panels) and the Bayes model averaged viscous posterior when the shear viscosity is constant with temperature (bottom panels). Individual 90% credible intervals for the Grad and Chapman-Enskog viscous corrections that underlie the averaging are shown in blue and red, respectively.

Constraints on shear and bulk viscosity.—The 90% credibility intervals for the shear and bulk viscosities, obtained from the Bayesian calibration of our multistage model of heavy-ion collisions to the LHC datasets listed in the previous section, are shown at the top of Fig. 1. Results are shown for both the Grad and the Chapman-Enskog model of the hydrodynamics-to-hadrons transition. The results are similar for both models. At low temperatures ($T \approx 150$ MeV), large values of the specific bulk viscosity ζ/s are disfavored; conversely, significant values of bulk viscosity are favored between temperatures of 200 and 300 MeV. For the specific shear viscosity η/s, the model-to-data comparison leads to intermediate values ≈ 0.1 to 0.2 with a modest temperature dependence. To obtain a single constraint from multiple models, we use Bayesian model averaging [33,49,65], which yields the orange (dark) band shown in Fig. 1.

The weak temperature dependence of η/s found in Fig. 1 indicates that good agreement with measurements can also be obtained using a constant value of the specific shear viscosity: $\eta/s = 0.137^{+0.025}_{-0.028}$ with Grad viscous corrections and $\eta/s = 0.125^{+0.021}_{-0.022}$ for the Chapman-Enskog viscous correction model, shown in the bottom row. This question goes beyond the temperature dependence of η/s and is directly related to the predictivity of the model. A model with a temperature-dependent shear viscosity will always be able to describe measurements as well or better than a model with a constant η/s (under the straightforward assumption that the prior of the temperature-dependent η/s includes the constant values). The more important question is: given the additional model flexibility from the temperature-dependent η/s, is there a statistically

meaningful difference in the model's agreement with data? Metrics that balance model predictivity and its degree of agreement with data are well known (see e.g. [66,67]). In this work, we use the Bayes factor, denoted "B", as in Ref. [15]. This is calculated by taking the ratio of the Bayes evidence—the denominator $p(d, I)$ in Bayes' theorem Eq. (2)—between two posterior distributions. Generally, logarithms of Bayes factor ($\ln B$) larger than 5 provide strong support that the new model parameters increased the model's predictivity, while values smaller than 1 suggest little gain in predictivity [68]. The Bayes factors we obtain are $\ln B = 0.3 \pm 0.2$ for our "Grad" hydrodynamics-to-hadron models, and $\ln B = 0.9 \pm 0.4$ for the Chapman-Enskog approximation; they suggest negligible gain in predictivity of the model between constant and temperature-dependent η/s when describing the current set of data, a result that had also been hinted in previous analyses [15].
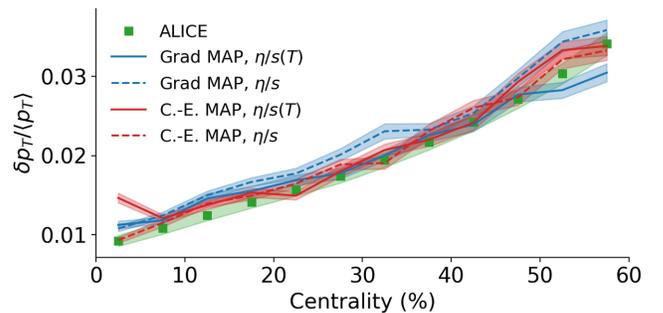
FIG. 2. Postdiction of $\delta p_T / \langle p_T \rangle$ at maximum *a posteriori*. Data from [37].
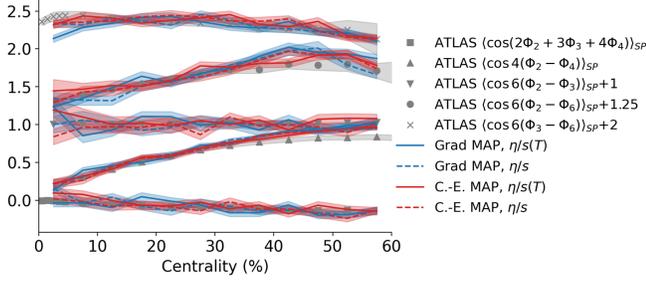
FIG. 3. Prediction of ATLAS event-plane correlations at maximum *a posteriori*. Data [40] and calculations are shifted for clarity.

In essence, the additional complexity of the model with a temperature-dependence η/s is not justified by the corresponding small improvement in describing experimental results; this suggests that models of heavy-ion collisions do not yet have the predictivity necessary to constrain the temperature dependence of the shear viscosity when the models' overall uncertainties are carefully accounted for.

The posterior for the viscosities, assuming a constant η/s, are shown in the bottom panels of Fig. 1. Constraints on the bulk viscosity are similar for both the constant and the temperature-dependent η/s. Confirming the results from the Bayes factor, we found a similar agreement with measurements for both the constant and temperature-dependent value of η/s shown in Fig. 1. This is shown in Fig. 2 for one of the measurements used for the calibration, the transverse momentum fluctuation. The results for a constant and a temperature-dependent η/s are consistent within statistical uncertainties. We verified that the same conclusion can be reached for all measurements used in the calibration (see Ref. [33]).

We now turn to comparison with measurements that were not used to constrain the viscosities and other model parameters. We first compare with event-plane correlations, which describe correlations between the symmetry axes of different Fourier harmonics [40,41]. As can be seen in Fig. 3, we find good agreement with four different event-plane correlators, with either model of hydrodynamics-to-hadrons transition and with either a constant η/s and a temperature-dependent one.
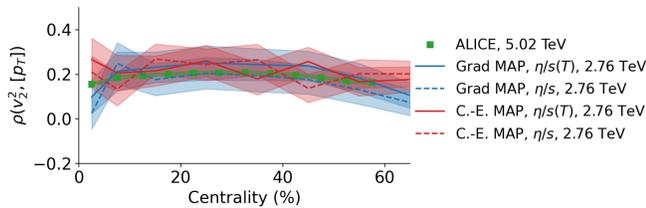
FIG. 4. Correlation between v_2^2 and p_T at maximum *a posteriori*, compared to data from a higher-energy collision. Note that data [69] are at $\sqrt{s_{NN}} = 5.02$ TeV while the maximum *a posteriori* predictions are at $\sqrt{s_{NN}} = 2.76$ TeV.

We further make a prediction for the correlation between momentum anisotropy fluctuations and average transverse momentum fluctuations, shown in Fig. 4. This observable was measured for $\sqrt{s_{NN}} = 5.02$ TeV Pb-Pb collisions by the ALICE [69] and ATLAS [70] collaborations. We make a prediction for $\sqrt{s_{NN}} = 2.76$ TeV Pb-Pb collisions, which we superimpose with the $\sqrt{s_{NN}} = 5.02$ TeV Pb-Pb collisions by the ALICE [69]. If, as expected, this observable is measured to have a very small $\sqrt{s_{NN}}$ dependence, we expect excellent agreement of our prediction with the measurement.

Summary.—We compared a multistage model of ultra-relativistic nuclear collisions to a large set of measurements from the Large Hadron Collider. By using the *ab initio* IP-Glasma model for the early stage of the collision combined with Bayesian inference techniques, we increased the model's predictivity, achieving excellent agreement with measurements used in the model-to-data comparisons, as well as additional measurements not used in the calibration. We found that our description of data remained robust even with a constant value for the shear viscosity over entropy density ratio η/s. The resulting model with a constant η/s and *ab initio* initial condition model has eight parameters, approximately *half* the number used in other modern multistage models of heavy-ion collisions, yet achieves a better agreement with data.

We carefully compared the results of our Bayesian analysis obtained with a temperature-dependent η/s or a constant value. We found no statistically meaningful improvement in the description of data between the two scenarios, suggesting that the model's predictivity is insufficient to constrain the shear viscosity's temperature dependence. We stress the importance of these statistical comparisons to understand if a model's improved agreement with data came at the cost of an increase in its complexity or an unreasonable weakening of its predictivity. In particular, improving agreement with data by adding parameters should not automatically lead to the conclusion that these new parameters are capturing important missing physics. To be very clear, these results do not imply that the specific shear viscosity has no temperature dependence: rather, our analysis and its components cannot statistically differentiate between the gentle slope obtained in one analysis and the flat one imposed in another.

Quantifying imperfections in our description of heavy-ion collisions is essential to obtaining robust extractions of the quark-gluon plasma's properties. Building upon previous work [64], we showed that the numerical cost of studying these theoretical uncertainties can be tamed by using modern computational techniques such as transfer learning. A much broader range of uncertainties can be explored in the near future, making possible a fuller picture of the transport coefficients of quantum chromodynamics.

[1] W. Busza, K. Rajagopal, and W. van der Schee, Heavy ion collisions: The big picture, and the big questions, Annu. Rev. Nucl. Part. Sci. **68**, 339 (2018).

[2] C. Gale, S. Jeon, and B. Schenke, Hydrodynamic modeling of heavy-ion collisions, Int. J. Mod. Phys. A **28**, 1340011 (2013).

[3] U. Heinz and R. Snellings, Collective flow and viscosity in relativistic heavy-ion collisions, Annu. Rev. Nucl. Part. Sci. **63**, 123 (2013).

[4] R. Derradi de Souza, T. Koide, and T. Kodama, Hydrodynamic approaches in relativistic heavy ion reactions, Prog. Part. Nucl. Phys. **86**, 35 (2016).

[5] P. Romatschke and U. Romatschke, *Relativistic Fluid Dynamics In and Out of Equilibrium*, Cambridge Monographs on Mathematical Physics (Cambridge University Press, Cambridge, England, 2019), 10.1017/9781108651998.

[6] P. Romatschke and U. Romatschke, Viscosity information from relativistic nuclear collisions: How perfect is the fluid observed at RHIC?, Phys. Rev. Lett. **99**, 172301 (2007).

[7] M. Luzum and P. Romatschke, Conformal relativistic viscous hydrodynamics: Applications to RHIC results at $\sqrt{s_{NN}} = 200$ GeV, Phys. Rev. C **78**, 034915 (2008); **79**, 039903(E) (2009).

[8] H. Petersen, C. Coleman-Smith, S. A. Bass, and R. Wolpert, Constraining the initial state granularity with bulk observables in Au + Au collisions at $\sqrt{s_{NN}} = 200$ GeV, J. Phys. G **38**, 045102 (2011).

[9] J. Novak, K. Novak, S. Pratt, J. Vredevoogd, C. E. Coleman-Smith, and R. L. Wolpert, Determining fundamental properties of matter created in ultrarelativistic heavy-ion collisions, Phys. Rev. C **89**, 034917 (2014).

[10] E. Sangaline and S. Pratt, Toward a deeper understanding of how experiments constrain the underlying physics of heavy-ion collisions, Phys. Rev. C **93**, 024908 (2016).

[11] J. E. Bernhard, P. W. Marcy, C. E. Coleman-Smith, S. Huzurbazar, R. L. Wolpert, and S. A. Bass, Quantifying properties of hot and dense QCD matter through systematic model-to-data comparison, Phys. Rev. C **91**, 054910 (2015).

[12] J. E. Bernhard, J. S. Moreland, S. A. Bass, J. Liu, and U. Heinz, Applying Bayesian parameter estimation to relativistic heavy-ion collisions: Simultaneous characterization of the initial state and quark-gluon plasma medium, Phys. Rev. C **94**, 024907 (2016).

[13] J. S. Moreland, J. E. Bernhard, and S. A. Bass, Bayesian calibration of a hybrid nuclear collision model using p-Pb and Pb-Pb data at energies available at the CERN Large Hadron Collider, Phys. Rev. C **101**, 024911 (2020).

[14] J. E. Bernhard, J. S. Moreland, and S. A. Bass, Bayesian estimation of the specific shear and bulk viscosity of quark–gluon plasma, Nat. Phys. **15**, 1113 (2019).

[15] D. Everett *et al.* (JETSCAPE Collaboration), Multisystem Bayesian constraints on the transport coefficients of QCD matter, Phys. Rev. C **103**, 054904 (2021).

[16] G. Nijs, W. van der Schee, U. Gürsoy, and R. Snellings, Transverse momentum differential global analysis of heavy-ion collisions, Phys. Rev. Lett. **126**, 202301 (2021).

[17] G. Nijs, W. van der Schee, U. Gürsoy, and R. Snellings, Bayesian analysis of heavy ion collisions with the heavy ion computational framework Trajectum, Phys. Rev. C **103**, 054909 (2021).

[18] G. Nijs and W. van der Schee, Predictions and postdictions for relativistic lead and oxygen collisions with the computational simulation code TRAJECTUM, Phys. Rev. C **106**, 044903 (2022).

[19] J. E. Parkkila, A. Onnerstad, and D. J. Kim, Bayesian estimation of the specific shear and bulk viscosity of the quark-gluon plasma with additional flow harmonic observables, Phys. Rev. C **104**, 054904 (2021).

[20] G. Nijs and W. van der Schee, A generalized hydrodynamizing initial stage for heavy ion collisions, arXiv:2304.06191.

[21] J. S. Moreland, J. E. Bernhard, and S. A. Bass, Alternative ansatz to wounded nucleon and binary collision scaling in high-energy nuclear collisions, Phys. Rev. C **92**, 011901(R) (2015).

[22] B. Schenke, P. Tribedy, and R. Venugopalan, Event-by-event gluon multiplicity, energy density, and eccentricities in ultrarelativistic heavy-ion collisions, Phys. Rev. C **86**, 034908 (2012).

[23] B. Schenke, P. Tribedy, and R. Venugopalan, Fluctuating Glasma initial conditions and flow in heavy ion collisions, Phys. Rev. Lett. **108**, 252301 (2012).

[24] L. D. McLerran and R. Venugopalan, Computing quark and gluon distribution functions for very large nuclei, Phys. Rev. D **49**, 2233 (1994).

[25] J. Bartels, K. J. Golec-Biernat, and H. Kowalski, A modification of the saturation model: DGLAP evolution, Phys. Rev. D **66**, 014001 (2002).

[26] H. Kowalski and D. Teaney, An impact parameter dipole saturation model, Phys. Rev. D **68**, 114005 (2003).

[27] C. Gale, S. Jeon, B. Schenke, P. Tribedy, and R. Venugopalan, Event-by-event anisotropic flow in heavy-ion collisions from combined Yang-Mills and viscous fluid dynamics, Phys. Rev. Lett. **110**, 012302 (2013).

[28] S. Ryu, J. F. Paquet, C. Shen, G. S. Denicol, B. Schenke, S. Jeon, and C. Gale, Importance of the bulk viscosity of QCD in ultrarelativistic heavy-ion collisions, Phys. Rev. Lett. **115**, 132301 (2015).

[29] S. McDonald, C. Shen, F. Fillion-Gourdeau, S. Jeon, and C. Gale, Hydrodynamic predictions for Pb + Pb collisions at 5.02 TeV, Phys. Rev. C **95**, 064913 (2017).

[30] S. Ryu, J.-F. Paquet, C. Shen, G. Denicol, B. Schenke, S. Jeon, and C. Gale, Effects of bulk viscosity and hadronic rescattering in heavy ion collisions at energies available at the BNL Relativistic Heavy Ion Collider and at the CERN Large Hadron Collider, Phys. Rev. C **97**, 034910 (2018).

[31] B. Schenke, C. Shen, and P. Tribedy, Running the gamut of high energy nuclear collisions, Phys. Rev. C **102,** 044905 (2020).

[32] C. Gale, J.-F. Paquet, B. Schenke, and C. Shen, Multi-messenger heavy-ion collision physics, Phys. Rev. C **105,** 014909 (2022).

[33] M. R. Heffernan, C. Gale, S. Jeon, and J.-F. Paquet, companion paper, Bayesian quantification of strongly interacting matter with color glass condensate initial conditions, Phys. Rev. C **109,** 065207 (2024).

[34] K. Aamodt *et al.* (ALICE Collaboration), Centrality dependence of the charged-particle multiplicity density at mid-rapidity in Pb-Pb collisions at $\sqrt{s_{NN}} = 2.76$ TeV, Phys. Rev. Lett. **106,** 032301 (2011).

[35] B. Abelev *et al.* (ALICE Collaboration), Centrality dependence of π, K, p production in Pb-Pb collisions at $\sqrt{s_{NN}} = 2.76$ TeV, Phys. Rev. C **88,** 044910 (2013).

[36] J. Adam *et al.* (ALICE Collaboration), Measurement of transverse energy at midrapidity in Pb-Pb collisions at $\sqrt{s_{NN}} = 2.76$ TeV, Phys. Rev. C **94,** 034903 (2016).

[37] B. B. Abelev *et al.* (ALICE Collaboration), Event-by-event mean p_T fluctuations in pp and Pb-Pb collisions at the LHC, Eur. Phys. J. C **74,** 3077 (2014).

[38] K. Aamodt *et al.* (ALICE Collaboration), Higher harmonic anisotropic flow measurements of charged particles in Pb-Pb collisions at $\sqrt{s_{NN}} = 2.76$ TeV, Phys. Rev. Lett. **107,** 032301 (2011).

[39] J. Adam *et al.* (ALICE Collaboration), Anisotropic flow of charged particles in Pb-Pb collisions at $\sqrt{s_{NN}} = 5.02$ TeV, Phys. Rev. Lett. **116,** 132302 (2016).

[40] G. Aad *et al.* (ATLAS Collaboration), Measurement of event-plane correlations in $\sqrt{s_{NN}} = 2.76$ TeV lead-lead collisions with the ATLAS detector, Phys. Rev. C **90,** 024905 (2014).

[41] S. Acharya *et al.* (ALICE Collaboration), Linear and non-linear flow modes in Pb-Pb collisions at $\sqrt{s_{NN}} = 2.76$ TeV, Phys. Lett. B **773,** 68 (2017).

[42] B. Schenke, S. Jeon, and C. Gale, $(3 + 1)$D hydrodynamic simulation of relativistic heavy-ion collisions, Phys. Rev. C **82,** 014903 (2010).

[43] B. Schenke, S. Jeon, and C. Gale, Elliptic and triangular flow in event-by-event $(3 + 1)$D viscous hydrodynamics, Phys. Rev. Lett. **106,** 042301 (2011).

[44] J.-F. Paquet, C. Shen, G. S. Denicol, M. Luzum, B. Schenke, S. Jeon, and C. Gale, Production of photons in relativistic heavy-ion collisions, Phys. Rev. C **93,** 044906 (2016).

[45] J. D. Bjorken, Highly relativistic nucleus-nucleus collisions: The central rapidity region, Phys. Rev. D **27,** 140 (1983).

[46] A. Bazavov *et al.* (HotQCD Collaboration), Equation of state in $(2 + 1)$-flavor QCD, Phys. Rev. D **90,** 094503 (2014).

[47] J. E. Bernhard, Bayesian parameter estimation for relativistic heavy-ion collisions, Ph.D. thesis, Duke University, 2018, arXiv:1804.06469.

[48] eosmaker, https://github.com/mrhheffernan/eos_maker/tree/smash/.

[49] D. Everett *et al.* (JETSCAPE Collaboration), Phenomenological constraints on the transport properties of QCD matter with data-driven model averaging, Phys. Rev. Lett. **126,** 242301 (2021).

[50] L. P. Csernai, J. I. Kapusta, and L. D. McLerran, On the strongly interacting low-viscosity matter created in relativistic nuclear collisions, Phys. Rev. Lett. **97,** 152303 (2006).

[51] J. Weil, V. Steinberg, J. Staudenmaier, L. G. Pang, D. Oliinychenko, J. Mohs, M. Kretz, T. Kehrenberg, A. Goldschmidt, B. Bäuchle, J. Auvinen, M. Attems, and H. Petersen, Particle production and equilibrium properties within a new hadron transport approach for heavy-ion collisions, Phys. Rev. C **94,** 054905 (2016).

[52] H. Grad, On the kinetic theory of rarefied gases, Commun. Pure Appl. Math. **2,** 331 (1949).

[53] W. Israel, Nonstationary irreversible thermodynamics: A causal relativistic theory, Ann. Phys. (N.Y.) **100,** 310 (1976).

[54] W. Israel and J. M. Stewart, Transient relativistic thermodynamics and kinetic theory, Ann. Phys. (N.Y.) **118,** 341 (1979).

[55] D. Teaney, The effects of viscosity on spectra, elliptic flow, and HBT radii, Phys. Rev. C **68,** 034913 (2003).

[56] K. Dusling, G. D. Moore, and D. Teaney, Radiative energy loss and v(2) spectra for viscous hydrodynamics, Phys. Rev. C **81,** 034907 (2010).

[57] A. Monnai and T. Hirano, Effects of bulk viscosity at freezeout, Phys. Rev. C **80,** 054906 (2009).

[58] K. Dusling and T. Schäfer, Bulk viscosity, particle spectra and flow in heavy-ion collisions, Phys. Rev. C **85,** 044909 (2012).

[59] G. S. Denicol, H. Niemi, E. Molnar, and D. H. Rischke, Derivation of transient relativistic fluid dynamics from the Boltzmann equation, Phys. Rev. D **85,** 114047 (2012); **91,** 039902(E) (2015).

[60] S. Chapman and T. G. Cowling, *The Mathematical Theory of Non-Uniform Gases: An Account of the Kinetic Theory of Viscosity, Thermal Conduction and Diffusion in Gases* (Cambridge University Press, Cambridge, England, 1990).

[61] J. Anderson and H. Witting, A relativistic relaxation-time model for the Boltzmann equation, Physica (Amsterdam) **74,** 466 (1974).

[62] A. Jaiswal, R. Ryblewski, and M. Strickland, Transport coefficients for bulk viscous evolution in the relaxation time approximation, Phys. Rev. C **90,** 044908 (2014).

[63] V. R. Joseph, E. Gul, and S. Ba, Maximum projection designs for computer experiments, Biometrika **102,** 371 (2015).

[64] D. Liyanage, Y. Ji, D. Everett, M. Heffernan, U. Heinz, S. Mak, and J.-F. Paquet, Efficient emulation of relativistic heavy ion collisions with transfer learning, Phys. Rev. C **105,** 034910 (2022).

[65] J. A. Hoeting, D. Madigan, A. E. Raftery, and C. T. Volinsky, Bayesian model averaging: A tutorial, Stat. Sci. **14,** 382 (1999).

[66] A. R. Liddle, How many cosmological parameters?, Mon. Not. R. Astron. Soc. **351,** L49 (2004).

[67] A. R. Liddle, Information criteria for astrophysical model selection, Mon. Not. R. Astron. Soc. **377,** L74 (2007).

[68] R. Trotta, Bayes in the sky: Bayesian inference and model selection in cosmology, Contemp. Phys. **49,** 71 (2008).

[69] S. Acharya *et al.* (ALICE Collaboration), Characterizing the initial conditions of heavy-ion collisions at the LHC with mean transverse momentum and anisotropic flow correlations, Phys. Lett. B **834,** 137393 (2022).

[70] G. Aad *et al.* (ATLAS Collaboration), Correlations between flow and transverse momentum in Xe + Xe and Pb + Pb collisions at the LHC with the ATLAS detector: A probe of the heavy-ion initial state and nuclear deformation, Phys. Rev. C **107**, 054910 (2023).

[71] For the specific shear viscosity, we use a piecewise linear function, with a low-temperature slope and a high-temperature slope separated by a single inflection point; the inflection point is often expected to be a minimum, as observed in the temperature dependence of other fluids [50], although we allow it to be either a minimum or a maximum. The specific bulk viscosity is parametrized with a skewed Cauchy distribution, allowing it to peak in the deconfinement region, and decrease at different rates above and below this peak. All details are in Ref. [33].